Lyotropic Supramolecular Helical Columnar Phases Formed by C3-Symmetric and Unsymmetric Rigid Molecules

ARTICLE *in* CHEMISTRY - A EUROPEAN JOURNAL · NOVEMBER 2012

Impact Factor: 5.73 · DOI: 10.1002/chem.201202944 · Source: PubMed

7 AUTHORS, INCLUDING:

Youju Huang
Chinese Academy of Sciences
49 PUBLICATIONS **397** CITATIONS
SEE PROFILE

Tsingze Xu
University of Science and Technology of Ch…
6 PUBLICATIONS **31** CITATIONS
SEE PROFILE

Liangbin Li
University of Science and Technology of Ch…
137 PUBLICATIONS **2,018** CITATIONS
SEE PROFILE

CHEMISTRY
A EUROPEAN JOURNAL

FULL PAPER

DOI: 10.1002/chem.201202944

Lyotropic Supramolecular Helical Columnar Phases Formed by C_3-Symmetric and Unsymmetric Rigid Molecules

Daoliang Wang, Youju Huang, Junjun Li, Lu Xu, Mingming Chen, Jiaojiao Tao, and Liangbin Li*[a]

Abstract: Unlike thermotropic liquid-crystalline C_3-symmetric molecules with flexible chains, the herein-designed fully rigid three-armed molecules (C_3-symmetric and unsymmetric) create a fancy architecture for the formation of lyotropic liquid crystals in water. First, hollow columns with triple-stranded helices, analogous to helical rosette nanotubes, are spontaneously constructed by self-organization of the rigid three-armed molecules. Then, the helical nanotubes arrange into hexagonal liquid-crystalline phases, which show macroscopic chirality as a result of supramolecular chiral symmetry breaking. Interestingly, the helical nanotubes constructed by the fully rigid molecules are robust and stable over a wide concentration range in water. They are hardly affected by ionic defects at the molecular periphery, that is, further decoration of functional groups on the molecular arms can presumably be realized without changing the helical conformation. In addition, the formed columnar phases can be aligned macroscopically by simple shear and show anisotropic ionic conductivity, which suggests promising applications for low-dimensional ion-conductive materials.

Keywords: chiral symmetry breaking · conducting materials · helical structures · liquid crystals · supramolecular chemistry

Introduction

Owing to molecular recognition, self-assembly and supramolecular function, supramolecular chemistry has been extensively studied in recent years and employed in various applications.[1] Particularly supramolecular liquid crystals, one of the most important branches of supramolecular chemistry, have gained increasing attention due to their complex superstructures and multiple functionalities.[2] By combining the hierarchical structures of supramolecular self-assembly and the unique properties of liquid crystals (e.g., molecular order and mobility), one can design various functional materials with desired performances.[2b,3] For example, low-dimensional ion-conductive materials were fabricated by using supramolecular liquid crystals.[4] Up to now, a great number of molecular building blocks with diverse geometrical shapes such as rod, fan, disk, cone and other exotic shapes[5] have been synthesized for the formation of supramolecular liquid crystals under thermotropic conditions.

Three-armed molecules (C_3-symmetric or unsymmetric) have received increasing attention in recent years due to their diverse functional arms and peculiar assembled structures.[6] Meijer and co-workers prepared C_3-symmetrical compounds for amplification of chirality in their supramolecular aggregates.[7] Molecules with C_3 symmetry are also used to construct metal–organic frameworks with wide applications like hydrogen storage and gas separation.[8] With the aid of flexible aliphatic chains, three-armed molecules are capable of programming supramolecular thermotropic liquid crystals.[9] However, to the best of our knowledge, there is no report on employing fully rigid three-armed molecules to establish supramolecular liquid crystals yet. With ionic groups at their periphery, fully rigid discoid[10] or plank-shaped (chromonic)[11] molecules can show special liquid-crystalline order in aqueous solution. In contrast to thermotropic liquid-crystalline C_3-symmetric molecules with flexible chains or chromonic liquid-crystalline molecules with plank shape, self-assembly of fully rigid three-armed molecules with ionic groups at their periphery faces the difficulty of filling the large void space among the individual arms. To minimize the contact between water molecules and the hydrophobic arms, the rigid three-armed molecules have to create a fancy architecture for the formation of lyotropic liquid crystal.

Herein, we designed and synthesized three fully rigid molecules to investigate the effects of topology and hydrophilicity on supramolecular assembly. These molecules with three-way rigid rod junctions (Scheme 1) have different numbers

[a] D. Wang,[+] Dr. Y. Huang,[+] J. Li, L. Xu, M. Chen, J. Tao, Prof. Dr. L. Li
National Synchrotron Radiation Lab and College of Nuclear Science and Technology
CAS Key Laboratory of Soft Matter Chemistry
Department of Polymer Science and Engineering
University of Science and Technology of China
No. 96, JinZhai Road, Hefei, Anhui, 230026 (P. R. China)
Fax: (+86) 551-5141078
E-mail: lbli@ustc.edu.cn

[+] These authors contributed equally to this work.

Supporting information for this article is available on the WWW under http://dx.doi.org/10.1002/chem.201202944.

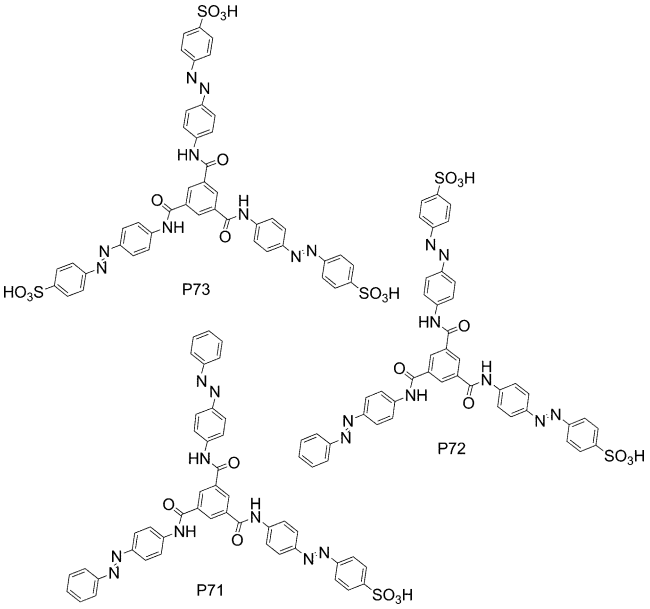

Scheme 1. Chemical structures of P73, P72, and P71.

of sulfo groups at their periphery, which lead to their corresponding C_3-symmetric and unsymmetric molecular structures. In the designations P73, P72 and P71, 7 represents the number of phenylene rings, indicating equally long arms in the molecules, and 1, 2 and 3 the number of ionic groups at the molecular periphery. Unexpectedly, P73, P72 and mixture P73/P71 spontaneously assemble into cylinders with triple-stranded helices in aqueous solution, which further arrange into hexagonal liquid-crystalline phases at high concentrations. The supramolecular helical cylinders can be aligned macroscopically by simple shear, which brings about anisotropic ionic conductivity in the liquid-crystalline phases.

Results and Discussion

Phase behavior of the liquid crystals: To explore how the ionic distributions and counterions affect the liquid-crystalline structures, three pure compounds (P73, P72 and P71), a complex of P73 and pyridine (1/2 molar ratio), denoted P73-Py, and a mixture of P73 and P71 (1/1 molar ratio), denoted P73/71, were studied. The liquid-crystalline behavior of these systems in water was studied by polarized optical microscopy (POM, Figure 1). With increasing concentration, solution, liquid-crystal (LC) and gel-like states were observed. Typical PO micrographs of the P73/water system are shown in Figure 2a (7 wt%, LC) and b (13 wt%, gel). At high concentration, the gel displays a stringlike texture and can be aligned by simple shear (Figure 2b). At low concentration, a transformation from gel to fluid liquid crystal takes place, which exhibits "tiger-skin" texture (Figure 2a). Similar textures are observed for the liquid-crystalline phases of other molecular systems (see Supporting Information S-Figure 1). Note that aggregates rather than monomers

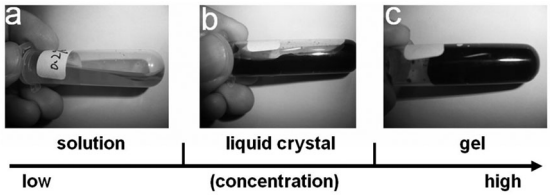

composition	P73	P73-Py	P72	P73/71	P71
liquid crystal (wt%)	5	4	2	2	NO
gel (wt%)	11	7.5	8	7	NO

Figure 1. Phase behaviors of various compositions in water at room temperature.

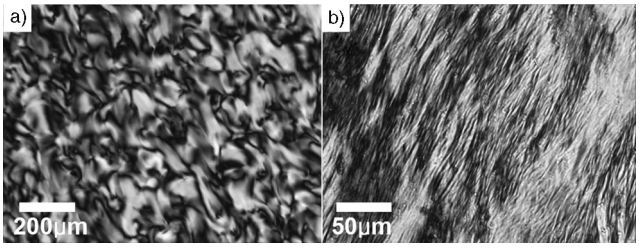

Figure 2. Polarizing optical micrographs of P73 in water at concentrations of a) 7 and b) 13 wt%.

are present in the solution states at low concentrations for these molecules, as verified by ^{1}H NMR measurements (see Supporting Information S-Figure 2).

The P72 system shows liquid-crystalline and gel states at lower concentrations than the P73 system, that is, the number of hydrophilic groups at the molecular periphery affects self-assembly. Compound P71 with one sulfo group cannot form a LC in water due to its low solubility ($\ll$1 wt%). With the same average number but different distribution of sulfo groups on the arms, the blended P73/71 system shows LC and gel states with concentrations (2 and 7 wt%) comparable to those of the P72 system (2 and 8 wt%). This indicates that the distribution of hydrophilic group on the arms barely affects the self-assembly behavior provided the average ionic density ensures sufficient solubility. The P73-Py system, which has pyridinium instead of proton as counterion, exhibits similar liquid-crystalline behavior with slightly lower concentrations for the LC and gel.

Structural characterization by SAXS and WAXS: To determine the supramolecular structures of all samples, synchrotron-based small- and wide-angle X-ray scattering (SAXS/WAXS) studies were performed at room temperature. All systems show scattering signals of hexagonal phases at sufficiently high concentrations, especially in their gel states. Figure 3a–c show representative two-dimensional SAXS and WAXS patterns of a hexagonal phase in a highly aligned sample, whereby the orientation direction is indicated by double-headed arrow. The corresponding one-dimensional diffraction curves for all systems at their gel concentrations are shown in Figure 3d (SAXS) and e (WAXS), in which the abscissa corresponds to the modulus of the scattering

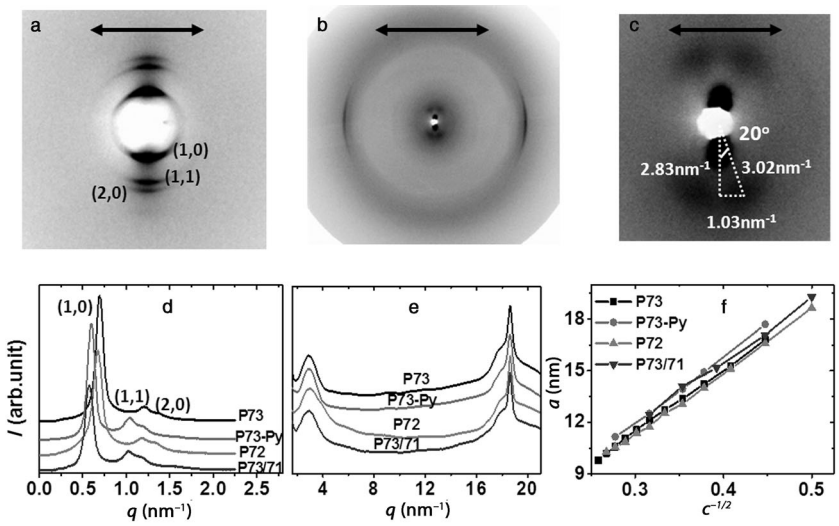

Figure 3. X-ray scattering patterns of aligned samples (arrow indicates shear direction). a) Small-angle region, b) wide-angle region and c) same as b), but medium-angle region. (d) 1D SAXS and (e) WAXS curves for different samples (P73: 13 wt%, P73-Py: 10 wt%, P72: 12 wt%, P73/71: 10 wt%). f) Relationship between concentration and spacing of adjacent columns in each sample system.

vector q. The three distinct diffraction peaks with a ratio of q values of $1:3^{1/2}:2$ and, moreover, an inconspicuous peak at $7^{1/2}$ lead to the conclusion that the liquid-crystalline phases of all investigated systems adopt hexagonal symmetry, and the three peaks can be indexed as (1,0), (1,1) and (2,0) (see Figure 3a and d). Orthogonal to the three major SAXS peaks, a sharp peak is observed for each system at a q value of 18.6 nm^{-1} in the wide-angle region (Figure 3b and e), which corresponds to a layer spacing of about 0.34 nm. These scattering data indicate long-range order for both in-plane and interlayer arrangements. In addition, four scattering points are spread around the vertical direction with a q value of 3.02 nm^{-1}, a phenomenon commonly regarded as fingerprint of helical structure, are observed in all systems (Figure 3c and e).

Decreasing the concentration of the three-armed molecules weakens the long-range order or decreases the correlation length of the hexagonal symmetry, which is manifested in broadening of the first-order peaks (1,0) and (1,1) as well as weakening of the second-order peak (2,0) in SAXS patterns (see Supporting Information S-Figure 3). Nevertheless, the hexagonal symmetries persist even at relatively low concentrations in all systems. Similar smooth transition of hexagonal phase was also observed in the P phases (hexagonal array), which were formed via the columns with effectively circular cross section in chromonic systems.[11b–d]

The q value of the (1,0) peak in all systems declines smoothly with decreasing concentration, whereas the peaks corresponding to the layer spacing at a q value of 18.6 nm^{-1} and helical structure at a q value of 3.02 nm^{-1} remain unchanged in position. In other words, increasing water content expands the distance among adjacent columns, but this does not affect the internal organization of the columns. This indicates that the columns are stable and robust, and cannot be easily broken by adding water. Based on the symmetry of hexagonal lattice, one can expect a linear dependence between the spacing between adjacent columns a and the reciprocal square root of the mass concentration $c^{-1/2}$. Our experimental results indeed coincide with this expectation (Figure 3f). All systems show good linear relations between a and $c^{-1/2}$ in the concentration range of the hexagonal phase. Furthermore, the molecular number in a single layer of columns can be derived from the linear slope, which is about three for all systems (see Supporting Information Part 3.1). Considering that even at very high concentration the spacing a ($\approx$10 nm) is far larger than the diameter of a single molecule ($\approx$3.5 nm, *trans* form of P73 molecule), it is reasonable for three molecules in a single layer to construct a column through layer-by-layer stacking, due to the coplanar configuration of P73 molecules. The *trans* form of P73 dominates in our system and the *cis* form is negligible, as was verified by UV/Vis spectra and ^{1}H NMR data (see Supporting Information S-Figure 5).

Symmetry breaking of supramolecular chirality: The X-ray data in Figure 3c suggest a helical conformation of columns. The CD spectra shown in Figure 4a further confirm helical structures in all systems. A bisignate signal with two Cotton effects around 330 and 375 nm and a crossover around 345 nm appears in each system, whereby the sign order reveals information about the chirality of supramolecular structure.[12] However, positive and negative (designated by the sign of the first long-wavelength band) bisignate CD signals both have a chance to show up in each system. For the sake of simplicity, Figure 4a shows selected CD curves for each system, while Figure 4b shows, for the example of the P73/water system at 5 wt% (or 8 wt%), that the CD curves can display positive (373/330 nm, +/−) or negative (373/330 nm, −/+) bisignate signals for different test batches. In view of the achiral P73 molecules, the CD signals mean that chiral symmetry breaking occurs in our LC systems, but in a spontaneous and unpredictable fashion.[13] Similar symmetry breaking of chirality has also been reported in other supramolecular aggregates of molecules involving ionic groups.[14] In addition, there are no obvious Cotton effects when the concentration (2 wt%) is far below the liquid-crystalline concentration (5 wt%). ^{1}H NMR studies show that P73 molecules exist as aggregates rather than monomers even at 1.5 wt% concentration (see Supporting Information S-Figure 2). Thus, the macroscopic chirality has a close relation with the ordered liquid-crystalline phase, because the

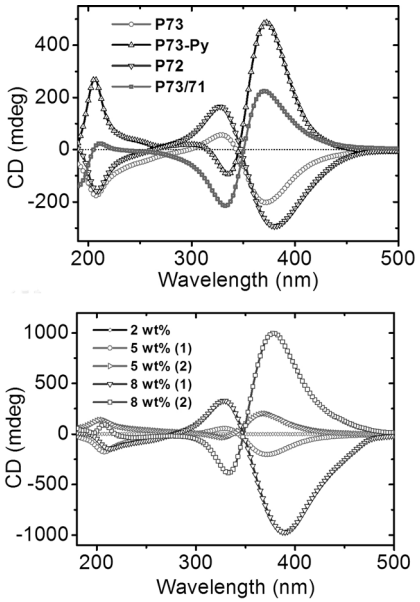

Figure 4. a) CD spectra of different samples at selected concentrations (P73: 5 wt%, P73-Py: 8 wt%, P72: 6 wt%, P73/71: 3 wt%). b) CD spectra of the P73/water systems at different concentrations; (1) and (2) represent different test batches.

independent aggregates are insufficient to induce symmetry breaking of chirality due to racemization.

Assembly model of the helical column: How do these rigid molecules assemble into a helical column? As shown in Figure 3c, the four scattering points have a 20° angle referring to the SAXS peaks of the in-plane hexagonal order (or 70° referring to the WAXS peak). The projection along the columnar axis gives $q = 3.02\cos 70° = 1.03\ \mathrm{nm}^{-1}$ in reciprocal space, which corresponds to a helical period of 6.10 nm along the columnar axis. As the columns have a layered structure with spacing of $0.34\ \mathrm{nm}^{-1}$, a helical period would contain 6.10/0.34 = 18 layers. That is, the first layer in a helical column would overlap geometrically with the 19th layer. Both the helical pitch and the layer spacing remain unchanged with varying molecular concentration, while the intercolumnar distance increases with decreasing concentration (see Supporting Information S-Figure 4). This suggests that the helical signal originates from intracolumn order, which is not affected by the interaction among columns.

To obtain a clear picture of the observed hexagonal phase, we reconstructed the electron density profile from the small-angle diffraction densities of the powder pattern (see Supporting Information Part 3.2). All systems show similar electron-density profiles for their hexagonal phases. Figure 5a shows the profile for P73/water system at 13 wt% concentration. The continuous regions of low electron density ($0.33\ \mathrm{e\,Å}^3$) correspond to water solvent, while the annuli of high density and central holes of intermediate density correspond to the helical columns and water channels, respectively. Based on this electron-density profile and X-ray and CD data, a schematic model for supramolecular helical column is given in Figure 5b (top view) and c (side view).

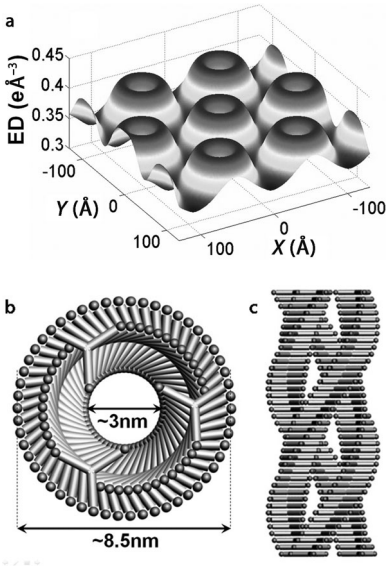

Figure 5. a) Electron-density profile of the 2D unit cell for P73/water system at a concentration of 13 wt%. Schematic representation of the supramolecular helical column in P73 system in b) top and c) side views.

From the top view, a water channel of about 3 nm and a columnar diameter of about 8.5 nm are present in a helical rosette nanotube. The fact that the diameter of the nanotube is close to the spacing a between adjacent columns at very high concentration suggests that the model is reasonable. From the side view, a triple-stranded helix is built up through layer-by-layer stacking, which gives the spiral and twining distribution of ions. Due to the periodic distribution of sulfo groups, anisotropic ionic conductivity is expected in the aligned hexagonal phase.

Anisotropic ionic conductivity: The ionic conductivities of the hexagonal phases were systematically studied and discussed here for the P73-Py system. Illustrations of cells for the conductivity measurements and POM images of oriented columns after simple shear are shown in S-Scheme 2 of the Supporting Information. As shown in Figure 6, the ionic conductivities in the direction parallel to the columnar axis ($\sigma_{\parallel}$, Figure 6P) are significantly higher than those in the direction perpendicular to the columnar axis ($\sigma_{\perp}$, Figure 6V), while the unaligned samples (Figure 6S) have ionic conductivities in between. At low concentrations where no liquid

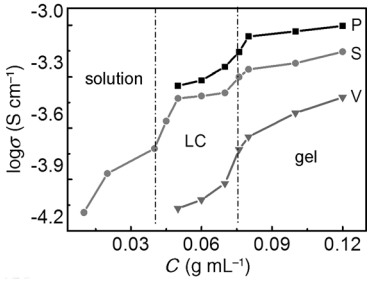

Figure 6. Ionic conductivities of P73-Py/water system at different concentrations parallel (P) and perpendicular (V) to the column axis and for an unaligned sample (S).

crystal phase forms, no anisotropic ionic conductivity is observed in the sheared samples, which further confirms the existence of aligned ionic nanochannels in the columnar phases. The columns in hexagonal phases are robust and stable over a wide concentration range, and thus promising for use as low-dimensional functional materials as have been successfully achieved for thermotropic liquid crystals.[3c,4,15]

Discussion: The helical rosette conformation is a new assembly mode for three-armed molecules, which often self-organize into single-stranded helical stacks according to previous literature.[7,21,6c] This unique triple-helical assembly of fully rigid three-armed molecules seems novel but is rather natural. It is well known that amphiphilic surfactants with a hydrophilic head and hydrophobic tails can self-organize into various well-defined nanoscale geometries in water, for example, micelles, vesicles and microtubules.[16] The triple-helical columns illustrated in Figure 5 are essentially microtubules. However, unlike flexible amphiphilic surfactants, which form microtubules with walls of liquid layers organized by flexible hydrophobic tails, the C_3-symmetrical or unsymmetrical molecules with rigid arms cannot pack freely to shield their hydrophobic rods from water. The triple-helical conformation seems the best choice to minimize contact between the arms and water, and also distributes the sulfo groups evenly on the interface. In addition, the directionality of hydrogen bonds also contributes to the helical columns according to previous literature.[16,12a,6b] There is no doubt that the triple-stranded helical structure is governed by a delicate balance among various interactions, such as dispersion forces, hydrophobic interactions, electrostatic forces and so on.[17,18a,19]

An interesting feature of our systems is that the supramolecular liquid crystals formed by achiral molecules show macroscopic chirality. Intensive studies on amplification of chirality in C_3-symmetrical molecules suggested that chirality of supramolecular aggregates emerged only when chiral substituents were introduced.[7] As mentioned above, successive rotation of the stacking molecules would produce a chiral column; however, this does not result in macroscopic chirality if the left- and right-handed columns are evenly distributed. The macroscopic chirality observed in our systems may stem from the cooperative interactions in the supramolecular liquid crystals, similar to the other symmetry-breaking systems.[13,18] Due to the cooperative interactions, the column formed at the very beginning will lead to the formation of a single-handedness domain. This is analogous to the autocatalytic pattern of primary seeding and secondary nucleation processes observed in sodium chlorate with chiral symmetry breaking.[18a,20] However, the handedness of the initiating column is randomly dominated, because the unit molecule is achiral. Hence we can obtain either levo- or dextrorotatory enantiomers, as is evidenced by the mirror-image CD curves (Figure 4b).

All of the experimental evidence suggests that the microtubules formed by the fully rigid three-armed molecules are robust. As indicated by X-ray scattering data, intracolumn order is not sensitive to variations in intercolumnar interaction. In contrast to aggregation of flexible amphiphilic molecules, which is driven by entropic changes, aggregation of the rigid three-armed molecules is mainly driven by enthalpy.[11] The strong interactions among adjacent arms (e.g., π–π interactions, hydrogen bonds) support the robustness of the microtubules. The robustness of the microtubules is also manifested in the same self-assembly behavior of the C_3-symmetric P73 and the unsymmetric P72 molecules. The C_3 symmetry of the P73 molecule allows a perfectly homogeneous distribution of sulfo groups at the surface of the microtubules. With only two sulfo groups, the unsymmetric configuration of the P72 molecule inherently introduces "ion defects" on the surface if we refer to P73 as the "perfect distribution". Clearly, the microtubules with strong interactions among the arms have high tolerance to ionic defects amounting to as much as one-third of the total ions, which is further confirmed by the same phase behavior of the P73/P71 blend. The high tolerance to ionic defects not only demonstrates the robustness of the microtubules but also suggests their versatility for further decoration on the arms without sulfo groups, which may permit us to endow the microtubules with diverse functions.

Conclusion

Fully rigid three-armed molecules can self-organize into supramolecular columnar liquid-crystalline phases with triple-helical rosette nanotubes as the columns, which are robust and stable over a wide concentration range in water. The helical nanotubes are hardly affected by ionic defects at the molecular periphery, and this would no doubt benefit further functionalization of their liquid crystals. The formed hexagonal phases exhibit two distinctive properties. First, the supramolecular helical cylinders can be aligned macroscopically by simple shear, which leads to anisotropic ionic conductivities in the hexagonal phases. Second, the ordered liquid-crystalline structures of organized achiral molecules showed macroscopic chirality, which indicates the occurrence of spontaneous chiral symmetry breaking in these systems. These interesting findings open the possibility to prepare low-dimensional ion-conductive materials and some other functional liquid-crystalline materials with single-handed helices based on only achiral molecules.

Experimental Section

Design and synthesis of three-armed molecules: materials, Synthetic details and characterization of all new compounds are given in Part 1 of the Supporting information.

Experimental instruments and methods: Olympus (Japan) BX-51-P microscope system was used to obtain polarizing optical micrographs. CD spectra were recorded on a Jasco J-810 spectropolarimeter. Ionic conductivities were measured by the alternating-current impedance method according to previous literature[15a] on a CHI660C electrochemistry work-

station (frequency range: 0.1 Hz to 100 kHz, applied voltage: 0.005 V). Some of the SAXS/WAXS measurements were performed on a synchrotron-radiation X-ray scattering station with a radiation wavelength of 0.154 nm and Mar 345 image plate as a detector at NSRL (China). Oriented samples were obtained by fluid shear in a 1 mm Kapton-film tube with a sample holder. As the area of the imaging plate cannot cover SAXS and WAXS data at a single sample-to-detector distance, the sample-to-detector distance was set at 400 and 200 mm to measure the SAXS and WAXS data, respectively, during which the sample was fixed on the sample holder without any movement. Some of the SAXS measurements were carried out by using an in-house setup with a 30 W micro X-ray source (Incoatec GmbH) and a multiwire proportional chamber detector (Bruker Hi-star). The radiation wavelength was 0.154 nm. The Fit2D software package was used to analyze the 2D SAXS/WAXS patterns.

Acknowledgements

The authors would like to thank Prof. Goran Ungar (Sheffield), Prof. Wim H. de Jeu (Amherst) and Prof. Lihua Yang (Hefei) for helpful discussions. This work is supported by the National Natural Science Foundation of China (51033004, 50973103, 51120135002 and 20904050), the Fund for One Hundred Talents of CAS, 973 program of MOST (2010CB934504) and the Fundamental Research Funds for the Central Universities. SAXS and WAXS measurements were done in NSRL and SSRF.

[1] a) J. M. Lehn, *Angew. Chem.* **1990**, *102*, 1347–1362; *Angew. Chem. Int. Ed. Engl.* **1990**, *29*, 1304–1319; b) J. M. Lehn, *Science* **2002**, *295*, 2400–2403; c) J. M. Lehn, *Chem. Soc. Rev.* **2007**, *36*, 151–160; d) S. Leininger, B. Olenyuk, P. J. Stang, *Chem. Rev.* **2000**, *100*, 853–907; e) S. T. Nguyen, D. L. Gin, J. T. Hupp, X. Zhang, *Proc. Natl. Acad. Sci. USA* **2001**, *98*, 11849–11850.

[2] a) F. J. M. Hoeben, P. Jonkheijm, E. W. Meijer, A. P. H. J. Schenning, *Chem. Rev.* **2005**, *105*, 1491–1546; b) C. Tschierske, *Chem. Soc. Rev.* **2007**, *36*, 1930–1970; c) T. Kato, N. Mizoshita, K. Kishimoto, *Angew. Chem.* **2006**, *118*, 44–74; *Angew. Chem. Int. Ed.* **2006**, *45*, 38–68; d) B. M. Rosen, M. Peterca, C. H. Huang, X. B. Zeng, G. Ungar, V. Percec, *Angew. Chem.* **2010**, *122*, 7156–7159; *Angew. Chem. Int. Ed.* **2010**, *49*, 7002–7005; e) V. Percec, M. N. Holerca, S. Nummelin, J. L. Morrison, M. Glodde, J. Smidrkal, M. Peterca, B. M. Rosen, S. Uchida, V. S. K. Balagurusamy, M. J. Sienkowska, P. A. Heiney, *Chem. Eur. J.* **2006**, *12*, 6216–6241; f) F. Camerel, B. Donnio, C. Bourgogne, M. Schmutz, D. Guillon, P. Davidson, R. Ziessel, *Chem. Eur. J.* **2006**, *12*, 4261–4274.

[3] a) S. A. Miller, E. Kim, D. H. Gray, D. L. Gin, *Angew. Chem.* **1999**, *111*, 3205–3210; *Angew. Chem. Int. Ed.* **1999**, *38*, 3021–3026; b) Y. Xu, W. Gu, D. L. Gin, *J. Am. Chem. Soc.* **2004**, *126*, 1616–1617; c) H. Sirringhaus, P. J. Brown, R. H. Friend, M. M. Nielsen, K. Bechgaard, B. M. W. Langeveld-Voss, A. J. H. Spiering, R. A. J. Janssen, E. W. Meijer, P. Herwig, D. M. de Leeuw, *Nature* **1999**, *401*, 685–688.

[4] a) M. Yoshio, T. Mukai, K. Kanie, M. Yoshizawa, H. Ohno, T. Kato, *Adv. Mater.* **2002**, *14*, 351–354; b) T. Kato, *Angew. Chem.* **2010**, *122*, 8019–8021; *Angew. Chem. Int. Ed.* **2010**, *49*, 7847–7848; c) J. Ruokolainen, R. Mäkinen, M. Torkkeli, T. Mäkelä, R. Serimaa, G. ten Brinke, O. Ikkala, *Science* **1998**, *280*, 557–560.

[5] a) M. Prehm, F. Liu, X. Zeng, G. Ungar, C. Tschierske, *J. Am. Chem. Soc.* **2011**, *133*, 4906–4916; b) B. M. Rosen, C. J. Wilson, D. A. Wilson, M. Peterca, M. R. Imam, V. Percec, *Chem. Rev.* **2009**, *109*, 6275–6540; c) F. Vera, J. Barberá, P. Romero, J. L. Serrano, M. B. Ros, T. Sierra, *Angew. Chem.* **2010**, *122*, 5030–5034; *Angew. Chem. Int. Ed.* **2010**, *49*, 4910–4914; d) H. K. Lee, H. Y. Lee, Y. H. Ko, Y. J. Chang, N. K. Oh, W. C. Zin, K. Kim, *Angew. Chem.* **2001**, *113*, 2741–2743; *Angew. Chem. Int. Ed.* **2001**, *40*, 2669–2671; e) C. V. Yelamaggad, G. Shanker, R. V. R. Rao, D. S. S. Rao, S. K. Prasad, V. V. S. Babu, *Chem. Eur. J.* **2008**, *14*, 10462–10471; f) J. J. van Gorp, J. A. J. M. Vekemans, E. W. Meijer, *J. Am. Chem. Soc.* **2002**, *124*, 14759–14769; g) A. Belaissaoui, I. M. Saez, S. J. Cowling, X. B. Zeng, J. W. Goodby, *Chem. Eur. J.* **2012**, *18*, 2366–2373.

[6] a) L. L. Lai, S. J. Hsu, H. C. Hsu, S. W. Wang, K. L. Cheng, C. J. Chen, T. H. Wang, H. F. Hsu, *Chem. Eur. J.* **2012**, *18*, 6542–6547; b) G. Argouarch, R. Veillard, T. Roisnel, A. Amar, H. Meghezzi, A. Boucekkine, V. Hugues, O. Mongin, M. Blanchard-Desce, F. Paul, *Chem. Eur. J.* **2012**; c) I. Danila, F. Riobe, F. Piron, J. Puigmarti-Luis, J. D. Wallis, M. Linares, H. Agren, D. Beljonne, D. B. Amabilino, N. Avarvari, *J. Am. Chem. Soc.* **2011**, *133*, 8344–8353; d) B. P. Dash, R. Satapathy, E. R. Gaillard, J. A. Maguire, N. S. Hosmane, *J. Am. Chem. Soc.* **2010**, *132*, 6578–6587.

[7] a) M. M. J. Smulders, A. P. H. J. Schenning, E. W. Meijer, *J. Am. Chem. Soc.* **2008**, *130*, 606–611; b) A. R. A. Palmans, E. W. Meijer, *Angew. Chem.* **2007**, *119*, 9106–9126; *Angew. Chem. Int. Ed.* **2007**, *46*, 8948–8968; c) P. J. M. Stals, J. C. Everts, R. de Bruijn, I. A. W. Filot, M. M. J. Smulders, R. Martín-Rapún, E. A. Pidko, T. F. A. de Greef, A. R. A. Palmans, E. W. Meijer, *Chem. Eur. J.* **2010**, *16*, 810–821.

[8] a) D. Zhao, D. J. Timmons, D. Yuan, H. C. Zhou, *Acc. Chem. Res.* **2011**, *44*, 123–133; b) J. K. Schnobrich, O. Lebel, K. A. Cychosz, A. Dailly, A. G. Wong-Foy, A. J. Matzger, *J. Am. Chem. Soc.* **2010**, *132*, 13941–13948.

[9] a) M. Lehmann, *Chem. Eur. J.* **2009**, *15*, 3638–3651; b) M. Lehmann, M. Jahr, F. C. Grozema, R. D. Abellon, L. D. A. Siebbeles, M. Müller, *Adv. Mater.* **2008**, *20*, 4414–4418; c) M. Lehmann, M. Jahr, *Chem. Mater.* **2008**, *20*, 5453–5456; d) D. Goldmann, D. Janietz, C. Schmidt, J. H. Wendorff, *Angew. Chem.* **2000**, *112*, 1922–1925; *Angew. Chem. Int. Ed.* **2000**, *39*, 1851–1854; e) D. Janietz, *J. Mater. Chem.* **1998**, *8*, 265–274.

[10] Y. Huang, Y. Cong, J. Li, D. Wang, J. Zhang, L. Xu, W. Li, L. Li, G. Pan, C. Yang, *Chem. Commun.* **2009**, 7560.

[11] a) S. W. Tam-Chang, L. M. Huang, *Chem. Commun.* **2008**, 1957–1967; b) J. Lydon, *J. Mater. Chem.* **2010**, *20*, 10071–10099; c) J. Lydon, *Curr. Opin. Colloid Interface Sci.* **2004**, *8*, 480–490 d) J. Lydon, *Curr. Opin. Colloid Interface Sci.* **1998**, *3*, 458–466.

[12] P. A. Korevaar, S. J. George, A. J. Markvoort, M. M. J. Smulders, P. A. J. Hilbers, A. P. H. J. Schenning, T. F. A. De Greef, E. W. Meijer, *Nature* **2012**, *481*, 492–496.

[13] a) X. Huang, C. Li, S. Jiang, X. Wang, B. Zhang, M. Liu, *J. Am. Chem. Soc.* **2004**, *126*, 1322–1323; b) Y. Qiu, P. Chen, M. Liu, *Langmuir* **2010**, *26*, 15272–15277.

[14] a) J. M. Ribó, J. Crusats, F. Sagués, J. Claret, R. Rubires, *Science* **2001**, *292*, 2063–2066; b) H. von Berlepsch, C. Bolttcher, A. Ouart, C. Burger, S. Dalhne, S. Kirstein, *J. Phys. Chem. B* **2000**, *104*, 5255–5262; c) Y. Qiu, P. Chen, M. Liu, *J. Am. Chem. Soc.* **2010**, *132*, 9644–9652.

[15] a) M. Yoshio, T. Mukai, H. Ohno, T. Kato, *J. Am. Chem. Soc.* **2004**, *126*, 994–995; b) M. Yoshio, T. Kagata, K. Hoshino, T. Mukai, H. Ohno, T. Kato, *J. Am. Chem. Soc.* **2006**, *128*, 5570–5577.

[16] D. L. Gin, W. Gu, B. A. Pindzola, W. J. Zhou, *Acc. Chem. Res.* **2001**, *34*, 973–980.

[17] J. van Herrikhuyzen, P. Jonkheijm, A. P. H. J. Schenning, E. W. Meijer, *Org. Biomol. Chem.* **2006**, *4*, 1539–1545.

[18] a) A. Pawlik, S. Kirstein, U. D. Rossi, S. Daehne, *J. Phys. Chem. B* **1997**, *101*, 5646–5651; b) X. Huang, M. Liu, *Chem. Commun.* **2003**, 66–67.

[19] J. H. K. K. Hirschberg, L. Brunsveld, A. Ramzi, J. A. J. M. Vekemans, R. P. Sijbesma, E. W. Meijer, *Nature* **2000**, *407*, 167–170.

[20] D. K. Kondepudi, K. V. Bullock, J. A. Digits, J. K. Hall, J. M. Miller, *J. Am. Chem. Soc.* **1993**, *115*, 10211–10216.

[21] F. García, P. M. Viruela, E. Matesanz, E. Ortí, L. Sánchez, *Chem. Eur. J.* **2011**, *17*, 7755–7759.

Received: August 17, 2012
Published online: November 14, 2012

